



HAL
open science

Time-delay Estimation based on an Enhanced Modified MUSIC with Co-prime Frequency Sampling for Rough Pavement

Biyun Ma, Zihui Liu, Cui Qiu, Jiaojiao Liu, Yide Wang, Hua Yu

► **To cite this version:**

Biyun Ma, Zihui Liu, Cui Qiu, Jiaojiao Liu, Yide Wang, et al.. Time-delay Estimation based on an Enhanced Modified MUSIC with Co-prime Frequency Sampling for Rough Pavement. IEEE Geoscience and Remote Sensing Letters, 2024, pp.3506805. 10.1109/LGRS.2024.3405177 . hal-04588386

HAL Id: hal-04588386

<https://hal.science/hal-04588386>

Submitted on 3 Jul 2024

HAL is a multi-disciplinary open access archive for the deposit and dissemination of scientific research documents, whether they are published or not. The documents may come from teaching and research institutions in France or abroad, or from public or private research centers.

L'archive ouverte pluridisciplinaire **HAL**, est destinée au dépôt et à la diffusion de documents scientifiques de niveau recherche, publiés ou non, émanant des établissements d'enseignement et de recherche français ou étrangers, des laboratoires publics ou privés.



Distributed under a Creative Commons Attribution - NonCommercial 4.0 International License

Time-delay Estimation based on an Enhanced Modified MUSIC with Co-prime Frequency Sampling for Rough Pavement

Biyun MA, Zhihui LIU, Cui QIU, Jiaojiao LIU, Yide WANG, (Senior Member, IEEE), Hua YU

Abstract—In cases involving a rough interface, the echo frequency behavior of ultrawideband GPR approximates a nonlinear Gaussian function. This characteristic leads to poor robustness and high computational complexity in existing modified MUSIC (Mod-MUSIC) methods. To address this challenge, this letter proposes an enhanced modified MUSIC (E-Mod-MUSIC) approach to mitigate the interference of false peaks, thus enhancing robustness. Furthermore, to reduce computational complexity while maintaining high estimation accuracy comparable to dense uniform frequency sampling structures, a distributed co-prime frequency sampling structure is employed with E-Mod-MUSIC. Numerical simulations with different scenarios show the effectiveness of the proposed method.

Index Terms—Ground Penetrating Radar (GPR), Interface Roughness, Time-Delay Estimation (TDE), Co-prime Frequency Sample.

I. INTRODUCTION

GROUND penetrating radar (GPR) is widely used in the fields of civil engineering to assess the quality of civil engineering materials, such as pavements, bridges, and tunnels [1], [2]. For pavement surveys, GPR is utilized for rapid data collection, the thickness measurement of layers, and the detection or the analysis of damage zones [3], [4]. In pavement survey, it is assumed that the pavement layers are horizontally stratified, and the vertical structure of the pavement can be determined through time-delay and amplitude estimations based on radar profiles [5].

In the rough interface case, the interface roughness has a great effect on the frequency behavior of the backscattered echoes. Layer interface reflections can be identified using the matched filter method for thickness determination [6]. When the center frequency is less than 2GHz, the frequency behavior of echoes is approximately an exponential function, so the covariance matrix does not satisfy the Vandermonde structure. Note that, Vandermonde structure of covariance matrix is mandatory for decorrelation techniques, such as spatial smoothing preprocessing (SSP). Some high-resolution methods, such as MUSIC and ESPRIT with improved SSP can be used for high-precision time-delay estimation (TDE)

for coherent echoes. While when the upper frequency of GPR ranges up to 8-10 GHz, as in ultrawideband GPR (UWB-GPR), the existing research shows that the echo frequency behavior of UWB-GPR is approximately a nonlinear Gaussian function [7], so the covariance matrix does not satisfy the Vandermonde structure. Therefore, SSP cannot be applied directly for decorrelation preprocessing in the UWB-GPR case.

There are some improved TDE methods considering the frequency behavior of the UWB-GPR case. In [8], a modified MUSIC combined with interpolation spatial smoothing (ISS) is used for TDE with unknown frequency behavior of echoes. ISS can transform the covariance matrix into a Vandermonde matrix to overcome the nonlinear frequency behavior. However, the computation load of this method is huge due to the additional rank-restore preprocessing procedures for the proper split of signal and noise subspace, because of the coherency of backscattered echoes [9]. To reduce the computation load, orthogonal matching pursuit (OMP) method [9], [10] is applied in the thickness estimation of pavement, and achieves good results in TDE. OMP methods are much more efficient than the ISS-based subspace methods, which do not require an additional decorrelation process to provide solutions for covariance matrix of the echo signal model that does not satisfy the sVandermonde structure. However, the resolution of OMP is limited by $1/BW$, where BW represents the sampling bandwidth of the GPR. In [10], the resolution of the method is improved to $1/2BW$ by extending the dictionary, but it is still noticeably inferior to methods such as MUSIC. Additionally, since the decrease in the amplitude of echoes along frequency is neglected in the dictionary of OMP, the model mismatch occurs in specific scenarios.

To address the high computational complexity arising from the nonlinear frequency behavior of UWB-GPR, this letter proposes a two-step method. Firstly, a distributed co-prime frequency sampling structure (DCFSS) is employed to reduce the number of sampling points, corresponding to a reduced number of points in the Fast Fourier Transform (FFT) of the echo signal and a decrease in the dimensionality of the covariance matrix. Secondly, an enhanced modified MUSIC (E-Mod-MUSIC) algorithm is applied to each frequency sampling subset to mitigate the interference from false peaks. Finally, the minimum description length (MDL) criterion and iterative steps are utilized to de-blur the results of the two sparse subsets. Numerical simulation results are presented to show the effectiveness and feasibility of the proposed method.

Thanks to the Natural Science Foundation of Guangdong Province of China under Grant No.2023A1515011420, 2022A1515011830, 2022A0505050011, and the French Agence Nationale de la Recherche (ANR) BeSensiCom project under Grant No.ANR-22-CE25-0002. Biyun MA, Zhihui LIU, Cui QIU, Jiaojiao LIU, and Hua YU are with the School of Electronics and Information Engineering, South China University of Technology, 510640 Guangzhou, China. Yide WANG is with the Institut d'Electronique et des Technologies du Numérique (IETR), CNRS UMR6164, Nantes University, 44306 Nantes, France. Corresponding author: Jiaojiao LIU (e-mail: jjliu@scut.edu.cn).

II. RECEIVED SIGNAL MODEL AND MOD-MUSIC

Assume that the studied media is considered only the first two or three typical thin asphalt pavement layers, which are low-loss media with negligible dispersivity, as indicated in [11]. The received signal model in the frequency domain is obtained by applying FFT to the echo signal in the time domain. Subsequently, considering the interface roughness, the frequency-domain signal is defined as follows, as in [8].

$$r(f) = \sum_{k=1}^K e(f) s_k(f) \exp(-j2\pi f t_k) + n(f) \quad (1)$$

where K is the number of echoes, which is assumed to be known or can be estimated by some detection criteria [12]. $e(f)$ is the radar pulse in the frequency domain. $s_k(f)$ represents the amplitude of the k th scattered echo, which can be divided into two parts, $s_k(f) = s_{rk} \varphi_k(f)$, where s_{rk} and $\varphi_k(f)$ are the reflection coefficient and the frequency behavior of the k th scattered echo, respectively. $n(f) \sim \mathcal{N}(0, \sigma^2)$ is the additive white Gaussian noise in frequency domain.

For N discrete frequencies with bandwidth B , (1) can be written as

$$\mathbf{r} = \mathbf{\Lambda} \mathbf{A} \mathbf{s} + \mathbf{n} \quad (2)$$

with the following notation definitions:

1) $\mathbf{r} = [r(f_1) r(f_2) \cdots r(f_N)]^T \in \mathbb{C}^{N \times 1}$ is the received signal vector in the frequency domain.

$$f_i = f_1 + (i-1)M\Delta f, i = 1, 2, \dots, N \quad (3)$$

f_1 is the lowest frequency, M can be any positive integer. In the scenario where a fixed frequency step Δf is given, the frequency sampling interval can be controlled by the parameter M . If M consists of two co-prime positive integers, two uniform frequency sampling subsets are obtained, then this frequency sampling scenario is referred to as DCFSS. Compared to DCFSS, when M is chosen to be only one integer, this scenario is referred to as uniform frequency sampling (UFS), particularly, when $M = 1$, it represents the densest UFS (D-UFS). The superscript T denotes the transpose operation.

2) $\mathbf{\Lambda} = \text{diag}\{e(f_1), e(f_2), \dots, e(f_N)\} \in \mathbb{C}^{N \times N}$ is the diagonal matrix composed of radar pulse $e(f)$.

3) $\mathbf{A} = [\mathbf{a}(t_1), \mathbf{a}(t_2), \dots, \mathbf{a}(t_K)] \in \mathbb{C}^{N \times K}$ is the mode matrix.

4) $\mathbf{a}(t_k) = [e^{-j2\pi f_1 t_k} \varphi_k(f_1), \dots, e^{-j2\pi f_N t_k} \varphi_k(f_N)]^T = \mathbf{A}_d(t_k) \boldsymbol{\varphi}_k \in \mathbb{C}^{N \times 1}$

5) $\mathbf{A}_d(t_k) = \text{diag}\{e^{-2j\pi f_1 t_k}, e^{-2j\pi f_2 t_k}, \dots, e^{-2j\pi f_N t_k}\} \in \mathbb{C}^{N \times N}$ is the diagonalized partial mode vector.

6) $\boldsymbol{\varphi}_k = [\varphi_k(f_1), \varphi_k(f_2), \dots, \varphi_k(f_N)]^T \in \mathbb{C}^{N \times 1}$ is the frequency behavior of the k th scattered echo, $\varphi_k(f)$ is real.

7) $\mathbf{s} = [s_{r1}, s_{r2}, \dots, s_{rK}]^T \in \mathbb{C}^{K \times 1}$ is the vector composed of the reflection coefficients of media.

8) $\mathbf{n} = [n(f_1), n(f_2), \dots, n(f_N)]^T \in \mathbb{C}^{N \times 1}$ is the noise vector with zero mean and covariance matrix $\sigma^2 \mathbf{I}_N$, where σ^2 is the noise power and $\mathbf{I}_N \in \mathbb{C}^{N \times N}$ is the identity matrix.

To facilitate the following process, the received signal vector is divided by $\mathbf{\Lambda}$, so \mathbf{r}_w can be written as

$$\mathbf{r}_w = \mathbf{\Lambda}^{-1} \mathbf{r} = \mathbf{A} \mathbf{s} + \mathbf{n}_w \quad (4)$$

where $\mathbf{n}_w = \mathbf{\Lambda}^{-1} \mathbf{n}$ is the noise vector after radar pulse whitening procedure. Then, the covariance matrix can be written as

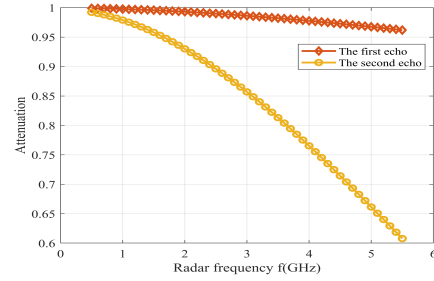


Fig. 1. The frequency behavior of first two echoes in rough interface model.

$$\mathbf{R} = E(\mathbf{r}_w \mathbf{r}_w^H) = \mathbf{A} \mathbf{S} \mathbf{A}^H + \sigma^2 \mathbf{\Sigma} \quad (5)$$

with $\mathbf{\Sigma} = \mathbf{\Lambda}^{-1} \mathbf{\Lambda}^{-H}$, $\mathbf{S} = \mathbf{s} \mathbf{s}^H$.

The rough interface with a Gaussian height probability density function and an exponential height autocorrelation function is modeled. In simulation, two distinct rough interfaces are considered, characterized by root mean square (RMS) heights, denoted as σ_h , of 1.0 mm and 2.0 mm, and correlation lengths, denoted as L_c , of 6.4 mm and 15 mm, respectively [8]. The propagation inside layer expansion (PILE) method was employed to generate the first two backscattered echoes at each frequency within the range $f \in [0.5, 5.5]$ GHz, with a sampling step of $\Delta f = 0.1$ GHz. As shown in Fig. 1, the interface roughness is characterized by a particular frequency signature of echo amplitudes, which decreases with frequency.

Therefore, to handle the nonlinearity of echo frequency behavior, the ISS technique is used to map the echo frequency behavior into an exponential function by an interpolation transformation matrix, and then the SSP is applied for decorrelation. After the interpolation procedure, the new covariance matrices can be written as follows

$$\bar{\mathbf{R}} = \mathbf{B} \mathbf{A} \mathbf{S} \mathbf{A}^H \mathbf{B}^H + \sigma^2 \mathbf{B} \mathbf{\Sigma} \mathbf{B}^H \quad (6)$$

where \mathbf{B} is the corresponding interpolation transformation matrix, as in [8]. To remove the contribution of colored noise $\sigma^2 \mathbf{B} \mathbf{\Sigma} \mathbf{B}^H$, the estimated noise variance $\hat{\sigma}^2$ is obtained by the eigenvalue decomposition (EVD) of covariance matrix, as in [13]. Assuming that the radar pulse and transformation matrix \mathbf{B} are known, the noise-free covariance matrices can be obtained

$$\bar{\mathbf{R}}_f = \bar{\mathbf{R}} - \hat{\sigma}^2 \mathbf{B} \mathbf{\Sigma} \mathbf{B}^H \approx \mathbf{B} \mathbf{A} \mathbf{S} \mathbf{A}^H \mathbf{B}^H + \mathbf{0} \quad (7)$$

Then, the covariance matrix after SSP is constructed as follows

$$\mathbf{R}_{\text{SSP}} = \frac{1}{M_{\text{SSP}}} \sum_{m=1}^{M_{\text{SSP}}} \bar{\mathbf{R}}_{f,m} \quad (8)$$

where $\bar{\mathbf{R}}_{f,m}$ represents the m th sub-band of the covariance matrix $\bar{\mathbf{R}}_f$. In (8), N frequencies and M_{SSP} overlapping sub-bands of length L are considered. N , M_{SSP} and L are constrained by $N = L + M_{\text{SSP}} - 1$, so the dimension of the \mathbf{R}_{SSP} is L .

In consequence, the pseudo-spectrum of Mod-MUSIC can be written as

$$P(t) = \begin{cases} \frac{\lambda_{(2)}(t)}{\lambda_{(1)}(t)} \cdots \frac{\lambda_{(L-1)}(t)}{\lambda_{(L-2)}(t)}, & L \text{ is odd} \\ \frac{\lambda_{(2)}(t)}{\lambda_{(1)}(t)} \cdots \frac{\lambda_{(L)}(t)}{\lambda_{(L-1)}(t)}, & L \text{ is even} \end{cases} \quad (9)$$

where $\lambda_{(n)}$ represents the n th small generalized eigenvalue of $\text{real}\{\mathbf{A}_d^H(t) \mathbf{U}_N \mathbf{U}_N^H \mathbf{A}_d(t)\}$ [8], \mathbf{U}_N is the noise subspace.

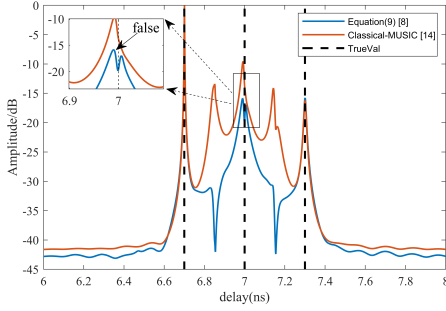


Fig. 2. Pseudo-spectrum of Mod-MUSIC and Classical-MUSIC for time delay estimation with SNR = 10dB, the three time delays are 6.7ns, 7.0ns and 7.3ns by uniform frequency sampling ranging from 0.5GHz to 5.5GHz with 91 frequency sampling points.

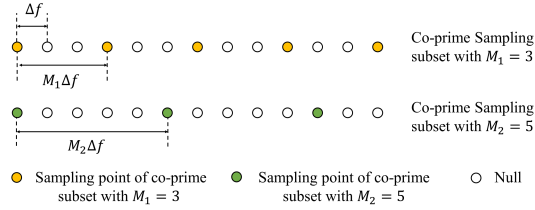


Fig. 3. A distributed co-prime sampling structure in the frequency domain.

III. TDE BY ENHANCED MOD-MUSIC WITH DCFSS

The Classical-MUSIC [14] pseudo-spectrum constructed by $P(t) = \frac{1}{\lambda_{(1)}(t)}$, where $\lambda_{(1)}(t)$ is the smallest eigenvalue, exhibits false peaks in the middle of true values. A Mod-MUSIC pseudo-spectrum constructed by (9) has a certain probability that the true value will also be canceled, resulting in two or more peaks appearing on both sides of the true value, as shown in Fig. 2. Therefore, in this section, E-Mod-MUSIC is proposed to avoid the interference of false peaks.

To elaborate, the first step involves selecting the candidate values by identifying the locations of all peaks in the pseudo-spectrum generated through Mod-MUSIC. Note that the candidate values contain false peaks. Subsequently, the K time delays are estimated from the candidate values based on the OMP method with the following steps. In each iteration, the best-fitting delay is obtained by Least Squares (LS) optimization, aiming to minimize the correlation with the residual signal. Then the chosen best-fitting delay is regarded as the final selection for that iteration, and the residual signal is updated by removing this delay and its corresponding contribution for the subsequent iteration. This iterative process is repeated for a total of K times, resulting in the acquisition of K estimated delays.

Furthermore, to address the high computational complexity due to the nonlinear frequency behavior of UWB-GPR, DCFSS is introduced. Fig. 3 illustrates an example of DCFSS, where the schematic diagram is shown for $M = 3$ and 5. In contrast to D-UFS with $M = 1$, DCFSS introduces a novel structure by conducting two separate FFT operations on the time-domain echo signals, utilizing the co-prime frequency intervals of two subsets. This approach reduces both the number of FFT points required for frequency sampling and the dimension of the covariance matrix of each frequency sampling subset.

However, when $M > 1$, sparse frequency sampling leads

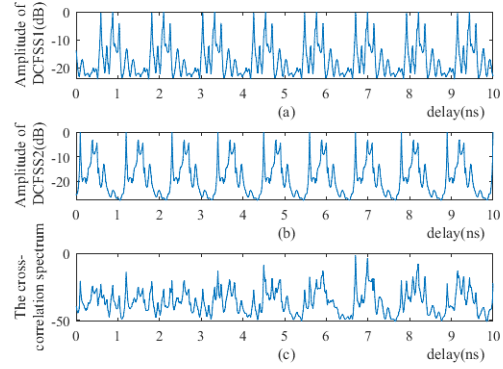


Fig. 4. Pseudo-spectrum of two co-prime frequency sampling subsets by Mod-MUSIC and its cross-correlation spectrum with time delay 6.7ns, 7.0ns, 7.3ns.

TABLE I
SAMPLING STRUCTURES IN FREQUENCY DOMAIN

Structures	f (GHz)	BW (GHz)	N
Subset1	[0.5: 0.42: 5.5]	5	$13(N_1)$
Subset2	[0.5: 0.463: 5.13]	4.63	$11(N_2)$
D-UFS	[0.5: 0.046: 5.5]	5	$109(N)$

to the pseudo-spectrum of Mod-MUSIC repeat periodically. To de-blur the results of the two subsets and improve the estimation accuracy, the cross-correlation spectrum of the pseudo-spectrums of two subsets is applied, which can be written as

$$P_{\text{crx}}(t) = \text{xcorr}(P_1(t), P_2(t)) \quad (10)$$

In Fig. 4, (a) and (b) show the pseudo spectrums of Mod-MUSIC of two subsets for time delay estimation with SNR = 0dB. Three true time delays are 6.7ns, 7.0ns, and 7.3ns, and the sparse frequency sampling range is from 0.5GHz to 5.5GHz, as shown in Table I; (c) is the cross-correlation spectrum of (a) and (b). In general, the cross-correlation spectrum suppresses the amplitude of periodically repeating false peaks and highlights the first true path. However, due to the noise and the false peaks, the number of peaks in the cross-correlation spectrum often exceeds the number of TDEs, and the peak corresponding to the first true path is not always the highest in the cross-correlation spectrum. To address this issue, the minimum description length (MDL) criterion [12], widely used in data compression with the maximum a posteriori (MAP) assumption, is applied to adaptively evaluate the number of valid peaks in the cross-correlation spectrum. The MDL equation for the cross-correlation spectrum of the two pseudo-spectrums of two subsets, denoted as $P_{\text{crx}}(t)$, is constructed as follows.

$$MDL(d) = - (N_t - d) J \log \left\{ \frac{\left(\prod_{i=d+1}^{N_t} P_{\text{crx}}(i) \right)^{\frac{1}{N_t-d}}}{\frac{1}{N_t-d} \sum_{i=d+1}^J P_{\text{crx}}(i)} \right\} \quad (11)$$

$$+ \frac{1}{2} d (2N_t - d) \log(J), d = 1 \cdots N_t$$

where N_t is the grid number of the pseudo-spectrum of MUSIC, J is the snapshot number. By minimizing (11), the value of d corresponding to the number of valid peaks in the cross-correlation spectrum is obtained. This value can be utilized to determine the candidate time-delay estimation range $\mathbf{t}_{\text{range}} = [\tau_1, \tau_1 + T)$, where τ_1 represents the estimated delay

Algorithm 1 Enhanced Mod-MUSIC with DCFSS.

Require: DCFSS subsets covariance matrix $\bar{\mathbf{R}}_1, \bar{\mathbf{R}}_2$ received data of both two subsets $\mathbf{r}_{w1}, \mathbf{r}_{w2}$, interpolation transform matrix $\mathbf{B}_1, \mathbf{B}_2$, the number of echoes K .

- 1: Apply ISS procedure to $\bar{\mathbf{R}}_1, \bar{\mathbf{R}}_2$ to attain $\mathbf{R}_{SSP1}, \mathbf{R}_{SSP2}$ by (6) and (8).
- 2: Calculate $P_1(t), P_2(t)$ by (9) and $P_{crx}(t)$ by (10).
- 3: Apply MDL to determine d by (11).
- 4: **if** $d == K$ **then**
- 5: Output the locations of d peaks in $P_{crx}(t)$ as $\hat{t}_k, k = 1, \dots, K$.
- 6: **else**
- 7: Calculate pseudo-spectra period T and determine the candidate delay range \mathbf{t}_{range} based on the locations of valid peaks by MDL criterion.
- 8: Apply peak search process to $P_1(t)$ or $P_2(t)$ within the candidate delay range to obtain $\hat{\tau} = \{\tau_i, i = 1, \dots, d\}$.
- 9: Initial residual signal $\mathbf{b} = \mathbf{r}_w$, iteration step $ii = 0$, selected mode matrix $\mathbf{W} = \emptyset$, selected amplitude vector $\mathbf{v} = \emptyset$, selected delay vector $\mathbf{t} = \emptyset, x = \mathbf{a}(\tau_i), i = 1, \dots, d$.
- 10: **while** $ii < K$ **do**
- 11: Find the index \hat{t}_m that solves the optimization problem: $\hat{t}_m = \underset{x}{\operatorname{argmax}} \{\min_x \|\mathbf{b}x - \mathbf{a}(\tau_i)\|\}$.
- 12: Update $\mathbf{W} = [\mathbf{W}, \mathbf{a}(\hat{t}_m)], \mathbf{v} = \mathbf{r}_w / \mathbf{W}, \mathbf{b} = \mathbf{r}_w - \mathbf{v}\mathbf{W}, \mathbf{t} = [\mathbf{t}, \hat{t}_m]$.
- 13: Let iteration step $ii = ii + 1$.
- 14: **end while**
- 15: **end if**

Ensure: Estimated delay $\hat{t}_k, k = 1, \dots, K$.

of the first path based on cross-correlation. The delay of the first valid cross-correlation peak and T is calculated by the pseudo-spectrum period of one subset. In the subsequent procedure, the pseudo-spectrum within the candidate estimation range is concerned, and the other estimated delays are selected by the proposed enhanced Mod-MUSIC algorithm. Therefore, the processing steps of the proposed method are outlined in Algorithm 1.

IV. SIMULATION RESULT AND ANALYSIS

The simulation results of the proposed E-Mod-MUSIC with DCFSS are presented in this section. Note that, the estimation of interface roughness has been extensively discussed in [8], which is not the primary focus of this letter. Fig. 5 shows that the backscattered echoes are reflected from a rough pavement composed of three random rough interfaces separating homogeneous media. The media is assumed to be non-dispersive. The sampling frequency is 0.5-5.5GHz. We evaluate the performance of the proposed method through a Monte Carlo process involving 100 independent runs of the algorithm with 100 independent noise snapshots. Two scenarios with different parameters of three primary echoes, as shown in Table II, are considered. The relative root mean square error (RRMSE) [15] is defined as,

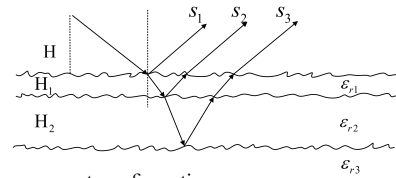


Fig. 5. Rough pavement configuration.

TABLE II
SIMULATION PARAMETERS IN SCENARIOS I AND II

Layer / Interface Parameter		Air	1	2	3
I	Relative Permittivity (ϵ_{rk})	1	4.5	7	9
	Thickness of layer (H_k , meter)	1.005	0.02	0.023	\
	Time of Arrival (t_k , ns)	6.7	7.0	7.3	\
	Roughness parameter (GHz^{-2})	0.016	0.017	0.03	\
II	Relative Permittivity (ϵ_{rk})	1	4.5	7	9
	Thickness of layer (H_k , meter)	1.005	0.02	0.026	\
	Time of Arrival (t_k , ns)	6.7	7.0	7.4	\
	Roughness parameter (GHz^{-2})	0.016	0.017	0.03	\

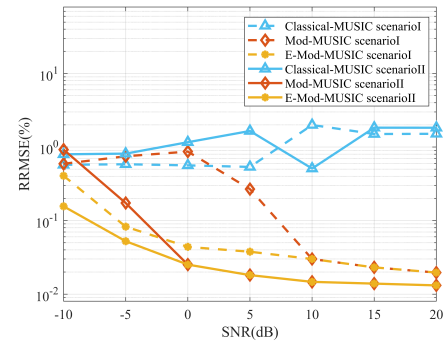


Fig. 6. RRMSEs of TDE versus the SNR with uniform frequency sampling in scenarios I and II.

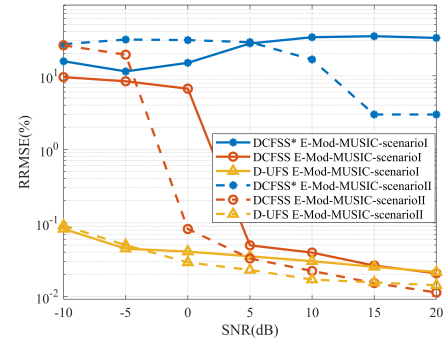


Fig. 7. RRMSEs of TDE versus the SNR with co-prime frequency sampling in scenarios I and II.

$$RRMSE = \frac{\sqrt{\sum_{k=1}^K \sum_{j=1}^Q (\hat{t}_{kj} - t_k)^2 / Q}}{t_{\min}} \quad (12)$$

where t_{kj} represents the estimated delay for the k th echo of the j th Monte Carlo run, Q is the number of Monte Carlo trials, and t_{\min} is the minimum time-delay of the detected echoes. The frequency sampling parameters are shown in Table I.

Firstly, the RRMSE performance of Classical-MUSIC [14], conventional modified MUSIC (Mod-MUSIC) [8], and the proposed E-Mod-MUSIC is compared with a D-UFS structure ($M = 1$). The RRMSEs of the time delays of the three coherent echoes in two scenarios are shown in Fig. 6.

In scenario I, where the time delay of the second echo is in the middle of the first and third one, the proposed E-Mod-MUSIC method with an additional selection procedure

works well in the region of low SNR and high SNR, but the performance of Mod-MUSIC is degraded due to more peaks appearing on both sides of the true value in the region of SNR less than 10dB, as shown in Fig. 6. It is indicated that the Mod-MUSIC is not as robust as E-Mod-MUSIC, which matches the statement mentioned in Fig. 2.

In scenario II, which is a normal case where the time delay of the second echo is not in the middle of the first and third one, the performance of E-Mod-MUSIC is as good as the Mod-MUSIC when SNR is more than 0dB. Moreover, Classical-MUSIC exhibits inadequate performance in both scenario I and scenario II due to the presence of false peaks amidst true values. It can be concluded that the robustness of the proposed E-Mod-MUSIC is superior to both Classical-MUSIC and Mod-MUSIC in different scenarios.

Secondly, to verify that the proposed enhanced method is still efficient under the co-prime frequency sampling structure, the performance of the proposed E-mod-MUSIC with DCFSS based on MDL criterion (11) (DCFSS E-Mod-MUSIC), the E-Mod-MUSIC with DCFSS constructed by (10) without MDL (DCFSS* E-Mod-MUSIC) and the E-Mod-MUSIC with densest uniform frequency sampling (D-UFS E-Mod-MUSIC) is compared as shown in Fig. 7. Owing to the notable reduction in sampling points, DCFSS* E-Mod-MUSIC exhibits inadequate performance. However, the proposed E-Mod-MUSIC with DCFSS, which evaluates the number of valid peaks by MDL criterion, outperforms the DCFSS* E-Mod-MUSIC in two scenarios. It is indicated that the MDL criterion, which can obtain the optimal representation model order of the cross-correlation by MAP Criterion, effectively evaluates the number of valid peaks in the cross-correlation spectrum adaptively, thereby facilitating the determination of the candidate time-delay estimation.

When the SNR exceeds 5dB, the proposed DCFSS E-Mod-MUSIC performs nearly as well as the D-UFS E-Mod-MUSIC in both scenarios. However, in scenario I, the performance of D-UFS E-Mod-MUSIC surpasses that of DCFSS E-Mod-MUSIC under low SNR conditions. Therefore, this trade-off is particularly valuable in the case of high SNR.

Furthermore, the computational complexity of the proposed DCFSS-based method is much lower than the densest uniform frequency sampling one. Since the minimum eigenvalue searching of Mod-MUSIC requires EVD for each frequency sampling on the pseudo-spectrum, the proposed algorithm with DCFSS has a computational complexity of $O(N_1 L_1^2 + N_2 L_2^2 + L_1^3 + L_2^3 + N_t(2L_1(L_1 - K) + 2L_2(L_2 - K)) + L_1 + L_2)$. In contrast, the Mod-MUSIC shows a computational complexity of $O(NL^2 + L^3 + N_t(2L(L - K) + L))$. For instance, Monte Carlo trials $Q = 100$ are experimented on a system with Windows 11, i5-12400, and Matlab R2023b. The running time of the proposed DCFSS-based method is $t_{\text{pro}} = 196\text{s}$, which significantly outperforms the modified MUSIC method, whose running time is $t_{\text{covn}} = 1623\text{s}$, achieving an average improvement rate of 87.9 %, defined as $(t_{\text{covn}} - t_{\text{pro}})/t_{\text{covn}} \times 100\%$.

V. CONCLUSION

In this letter, we have addressed the degraded performance of Mod-MUSIC in certain possible scenarios. To enhance

robustness, an enhanced modified MUSIC (E-Mod-MUSIC) involving iterations to select the candidate values by LS optimization is proposed. Additionally, to reduce the computation complexity while considering the interface roughness for UWB-GPR, a DCFSS with E-Mod MUSIC is introduced. Finally, to de-bur the results of two subsets, the MDL criterion is used to adaptively evaluate the number of valid peaks of the cross-correlation spectrum, thereby improving estimation performance. The numerical simulations with different scenarios show that, due to the additional selection procedure based on the MDL criterion, the proposed method exhibits better robustness than the existing methods, such as Classical-MUSIC and Mod-MUSIC.

REFERENCES

- [1] M. Sun, J. Pan, C. L. Bastard, Y. Wang, and J. Li, "Advanced signal processing methods for ground-penetrating radar: Applications to civil engineering," *IEEE Signal Processing Magazine*, vol. 36, no. 4, pp. 74–84, 2019.
- [2] M. Ambrosiano, M. Bevacqua, T. Isernia, and V. Pascazio, "The tomographic approach to ground-penetrating radar for underground exploration and monitoring: A more user-friendly and unconventional method for subsurface investigation," *IEEE Signal Processing Magazine*, vol. 36, no. 4, pp. 62–73, 2019.
- [3] D. H. Chen, F. Hong, W. Zhou, and P. Ying, "Estimating the hotmix asphalt air voids from ground penetrating radar," *NDT & E International*, vol. 68, pp. 120–127, 2014.
- [4] D. Kurrant and E. Fear, "Technique to decompose near-field reflection data generated from an object consisting of thin dielectric layers," *IEEE Transactions on Antennas and Propagation*, vol. 60, no. 8, pp. 3684–3692, 2012.
- [5] S. Wang, S. Zhao, and I. L. Al-Qadi, "Real-time density and thickness estimation of thin asphalt pavement overlay during compaction using ground penetrating radar data," *Survys in Geophysic*, vol. 41, no. 3, SI, pp. 431–445, MAY 2020.
- [6] S. Wang, Z. Leng, Z. Zhang, and X. Sui, "Automatic asphalt layer interface detection and thickness determination from ground-penetrating radar data," *Construction and Building Materials*, vol. 357, p. 129434, 2022.
- [7] M. Sun, C. L. Bastard, N. Pinel, Y. Wang, and J. Li, "Road surface layers geometric parameters estimation by ground penetrating radar using estimation of signal parameters via rotational invariance techniques method," *IET Radar Sonar Navigation*, vol. 10, no. 3, pp. 603–609, 2016.
- [8] M. Sun, C. L. Bastard, N. Pinel, Y. Wang, J. Li, J. Pan, and Z. Yu, "Estimation of time delay and interface roughness by GPR using modified MUSIC," *Signal Processing*, vol. 132, pp. 272–283, 2017.
- [9] M. Sun, J. Pan, Y. Wang, S. Member, X. Zhang, X. Xiao, C. Fauchard, and C. L. Bastard, "Time-delay estimation by enhanced orthogonal matching pursuit method for thin asphalt pavement with similar permittivity," *IEEE Transactions on Intelligent Transportation Systems*, vol. 23, no. 4, pp. 8940–8948, 2022.
- [10] J. Pan, M. Sun, Y. Wang, C. L. Bastard, and V. Baltazart, "Time-delay estimation by a modified orthogonal matching pursuit method for rough pavement," *IEEE Transactions on Geoscience and Remote Sensing*, vol. 59, no. 4, pp. 2973–2981, 2021.
- [11] C. L. Bastard, V. Baltazart, Y. Wang, and J. Saillard, "Thin-pavement thickness estimation using GPR with high-resolution and superresolution methods," *IEEE Transactions on Geoscience and Remote Sensing*, vol. 45, no. 8, pp. 2511–2519, 2007.
- [12] M. Wax and I. Ziskind, "Detection of the number of coherent signals by the MDL principle," *IEEE Transactions on Acoustics, Speech, and Signal Processing*, vol. 37, no. 8, pp. 1190–1196, 1989.
- [13] P. Stoica, T. Söderström, and V. Simonyundefined, "On estimating the noise power in array processing," *Signal Process.*, vol. 26, no. 2, p. 205–220, 1992.
- [14] F. Ge, D. Shen, Y. Peng, and V. O. K. Li, "Super-resolution time delay estimation in multipath environments," *IEEE Transaction on Circuits and Systems*, vol. 54, no. 9, pp. 1977–1986, SEP 2007.
- [15] H. Pan, J. Pan, and X. Zhang, "Time-delay estimation of coherent GPR signal by using sparse frequency sampling and IMUSIC method," in *2022 International Symposium on Wireless Communication Systems (ISWCS)*, 2022, pp. 1–6.